European Journal of Radiology 84 (2015) 1516–1524

Contents lists available at ScienceDirect

European Journal of Radiology

journal homepage: www.elsevier.com/locate/ejrad

Microvascular obstruction on delayed enhancement cardiac magnetic resonance imaging after acute myocardial infarction, compared with myocardial ^{201}Tl and ^{123}I-BMIPP dual SPECT findings

Hiroaki Mori[a,b], Satoshi Isobe[a,*], Shinichi Sakai[b], Takashi Yamada[a], Naoki Watanabe[b], Manabu Miura[b], Yasuhiro Uchida[c], Masaaki Kanashiro[c], Satoshi Ichimiya[c], Takahiro Okumura[a], Toyoaki Murohara[a]

[a] Department of Cardiology, Nagoya University Graduate School of Medicine, Nagoya, Japan
[b] Department of Cardiology, Kainan Hospital, Yatomi, Japan
[c] Department of Cardiology, Yokkaichi Municipal Hospital, Yokkaichi, Japan

ARTICLE INFO

Article history:
Received 24 December 2014
Received in revised form 30 March 2015
Accepted 4 May 2015

Keywords:
Microvascular obstruction
Magnetic resonance imaging
^{201}Tl and ^{123}I-BMIPP dual SPECT
Acute myocardial infarction

ABSTRACT

Background: The hypo-enhanced regions within the hyper-enhanced infarct areas detected by cardiac magnetic resonance (CMR) imaging reflect microvascular obstruction (MO) after acute myocardial infarction (AMI). The combined myocardial thallium-201 (^{201}Tl)/iodine-123-15-(p-iodophenyl)-3-(R,S)-methylpentadecanoic acid (^{123}I-BMIPP) dual single-photon emission computed tomography (SPECT) is a useful tool for detecting myocardial reversibility after AMI. We evaluated whether MO could be an early predictor of irreversible myocardial damage in comparison with ^{201}Tl and ^{123}I-BMIPP dual SPECT findings in AMI patients.

Methods: Sixty-two patients with initial AMI who successfully underwent coronary revascularization were enrolled. MO was defined by CMR imaging. Patients were divided into 2 groups as follows: MO group ($n = 32$) and non-MO group ($n = 30$). Scintigraphic defect scores were calculated using a 17-segment model with a 5-point scoring system. The mismatch score (MMS) was calculated as follows: the total sum of (Σ) ^{123}I-BMIPP defect score minus Σ^{201}Tl defect score. The percentage mismatch score (%MMS) was calculated as follows: MMS/(Σ^{123}I-BMIPP score) $\times$ 100 (%).

Results: The percentage infarct size (%IS) was significantly greater in the MO group than in the non-MO group (32.2 $\pm$ 13.8% vs. 18.3 $\pm$ 12.1%, $p < 0.001$). The %MMS significantly correlated with the %IS and the percentage MO ($r = -0.26$, $p = 0.03$; $r = -0.45$, $p < 0.001$, respectively). The %MMS was significantly greater in the non-MO group than in the MO group (45.4 $\pm$ 42.4% vs. 13.3 $\pm$ 28.0%, $p = 0.001$), and was an independent predictor for MO (OR 0.97, 95%CI 0.94–0.99, $p = 0.02$).

Conclusions: Our results reconfirm that, in comparison with myocardial dual scintigraphy, MO is an important structural abnormality. CMR imaging is useful for the early detection of irreversible myocardial damage after AMI.

Abbreviations: AMI, acute myocardial infarction; ^{123}I-BMIPP, iodine-123-15-(p-iodophenyl)-3-(R,S)-methylpentadecanoic acid; CMR, cardiac magnetic resonance; IS, infarct size; LGE, late gadolinium enhancement; LV, left ventricular; MMS, mismatch score; MO, microvascular obstruction; PCI, percutaneous coronary intervention; SPECT, single-photon emission computed tomography; ^{201}Tl, thallium-201.

* Corresponding author at: Department of Cardiology, Nagoya University Graduate School of Medicine, 65 Tsurumai-cho, Showa-ku, Nagoya 466-8560, Japan. Tel.: +81 52 744 2147; fax: +81 52 744 2138.
E-mail address: sisobe@med.nagoya-u.ac.jp (S. Isobe).

http://dx.doi.org/10.1016/j.ejrad.2015.05.002
0720-048X/

1. Introduction

Percutaneous coronary intervention (PCI) is one of the most effective contemporary therapies for reducing myocardial damage and ameliorating prognoses in patients with acute myocardial infarction (AMI). Despite the progress in therapeutic strategies for AMI, no-reflow is an afflicted phenomenon that leads to myocardial remodeling and poor outcomes in AMI patients [1,2]. Accordingly, early detection of myocardial irreversible damage due to no-reflow is crucial.

Cardiac magnetic resonance (CMR) imaging is a useful modality for assessing myocardial structural changes in AMI patients [3,4]. The hypo-enhanced regions within the hyper-enhanced infarct areas detected by CMR imaging are considered to correspond to microvascular obstruction (MO) [5–8]. MO is a stronger independent predictor of contractile recovery in the infarct zone than infarct volume or transmural extent [9]. Patients with AMI exhibiting MO are reported to have poor prognoses [10].

Radioisotope imaging is also a noninvasive, useful tool for detecting myocardial viability after AMI. Myocardial ^{201}Tl and ^{123}I-BMIPP dual scintigraphy enable simultaneous assessment of myocardial flow and fatty acid metabolism [11]. The areas exhibiting a flow-metabolism mismatch, defined as a larger defect on ^{123}I-BMIPP than that on ^{201}Tl, correspond to impaired but viable myocardium after AMI [12,13], and are considered to be where further improvements in myocardial function will be [14–17]. On the other hand, AMI patients showing a concordant defect on ^{201}Tl/^{123}I-BMIPP dual single-photon emission computed tomography (SPECT) have a worse outcome than those without it [17–20]. To the best of our knowledge, no data are available on the pathophysiological relationship between the structural changes on CMR imaging and flow-metabolism findings on dual SPECT in AMI patients.

In the present study, we examined the above-mentioned relationship and determined whether MO could be an early predictor for irreversible myocardial damage, in comparison with ^{201}Tl/^{123}I-BMIPP dual SPECT findings in AMI patients who successfully underwent emergency PCI.

2. Methods

2.1. Patient population

Patients who underwent successful emergency PCI for initial AMI, CMR imaging, and myocardial ^{201}Tl/^{123}I-BMIPP dual SPECT were retrospectively analyzed between October 2010 and May 2013. CMR imaging and dual SPECT in AMI patients were routinely performed in our institution. Eighty-three patients were enrolled at the entry of this study. The following patients were excluded: those with cardiac death ($n = 3$); atrial fibrillation ($n = 2$); or chronic kidney disease (serum creatinine level >1.5 mg/dL) ($n = 7$). Patients who were unable to follow breath-hold commands during CMR because of severe congestive heart failure ($n = 7$), chronic obstructive pulmonary disease ($n = 1$), or high age (>90 years) ($n = 1$) were also excluded. Finally, 62 patients (55 men and 7 women; mean age, 62 ± 12 years; age range, 32–86 years) were evaluated.

Acute myocardial infarction was diagnosed as the presence of typical anterior chest pain for at least 30 min, with ST segment elevation/depression in at least two contiguous electrocardiographic leads, and a > 2-fold creatine kinase elevation above the maximum peak in the normal range and/or serum troponin I elevation (>0.03 μg/L).

The study protocol was approved by the Ethical Committee of Kainan Hospital and informed consent was obtained from all patients.

2.2. Emergency PCI

Immediately after being diagnosed as AMI by electrocardiography, patients were given oral aspirin (200 mg). In accordance with a previous study [21], 12 mg doses of nicorandil dissolved in 100 mL of 0.9% saline were intravenously injected for 20–30 min at the initiation of emergency coronary angiography. After arterial access was achieved, intravenous heparin (3000 IU) was given. All patients underwent coronary angiography to confirm the target vessel, followed by PCI treatments with thrombectomy and/or coronary stent through the femoral artery. An added 7000 U of heparin was injected prior to PCI. All patients underwent PCI successfully with a residual stenosis of <30% at the target lesion. All patients were given aspirin (100 mg) and clopidogrel (75 mg) for at least 6 months after stent implantation. Coronary slow flow phenomenon was defined as follows [22]: (1) no evidence of obstructive epicardial coronary artery disease; (2) delayed distal vessel contrast opacification as evidenced by either Thrombolysis In Myocardial Infarction (TIMI) 2 flow or a corrected TIMI frame count >27 frames; and (3) delayed distal vessel opacification in at least 1 epicardial vessel.

2.3. Myocardial dual SPECT

Myocardial ^{201}Tl/^{123}I-BMIPP dual SPECT was conducted 10.4 ± 4.1 days after the onset of AMI. All patients underwent overnight fast and were suspended from cardiac medications for at least 24 h. One hundred and eleven MBq ^{201}Tl and 111 MBq ^{123}I-BMIPP were injected intravenously, and myocardial ^{201}Tl/^{123}I-BMIPP dual SPECT imaging was performed 10 min after tracer injection using a dual-head gamma camera (PICKER PRISM 2000 XP, Shimadzu Corporation, Kyoto, Japan) equipped with low-energy high-resolution collimators. The data were acquired over 180° in 6 steps of 40 s each on a 64 × 64 matrix. To separate the distribution of the isotopes, ^{201}Tl data were obtained using a symmetrical 68 keV with a 10% window, whereas ^{123}I-BMIPP data were captured using a symmetrical 159 keV with a 10% window. The three tomograms of vertical long, horizontal long, and short axis views were created using a dedicated software, Odyssey VP (Picker International Inc., Cleveland, OH). Images were reconstructed by filtered back-projection with a Low Pass filter (order 5, cut-off frequency 0.41 cycle/cm for both ^{201}Tl and ^{123}I-BMIPP images).

Scintigraphic defect scores were calculated using a 17-segment model with a 5-point scoring system on the polar map images, according to the recommendations of the American Heart Association, using a commercially available software (Heart Score View, Nihon Medi-Physics Co. Ltd., Tokyo, Japan) [23]. The mismatch score was calculated by subtracting the total sum of the ^{123}I-BMIPP and ^{201}Tl defect scores in each segment (Σ^{123}I-BMIPP defect score minus Σ^{201}Tl defect score). The percentage mismatch score (%MMS) was calculated as follows: %MMS = MMS/Σ^{123}I-BMIPP score × 100 (%).

2.4. CMR imaging

Cardiac magnetic resonance imaging was conducted 9.9 ± 4.1 days after the onset of AMI. All CMR studies were performed on a 1.5 T whole-body magnetic resonance scanner (Achieva Intera; Philips Healthcare, Best, The Netherlands) with an 8-element surface coil. The MRI protocol used an ECG-triggered breath-hold segmented steady-state free precession.

Two CMR sequences were used as follows: cine sequences were acquired with the following parameters: repetition time, 2.8 ms; echo time, 1.42 ms; slice thickness, 10 mm; no gap between slice; flip angle, 55; field of view, 350 × 350 mm; matrix, 192 × 256;

Table 1
Baseline characteristics of patients with and without MO.

Characteristic	All patients ($n=62$)	MO group ($n=32$)	Non-MO group ($n=30$)	p value
Male (%)	51 (82)	29 (90)	22 (86)	0.46
Age (years)	63 ± 12	60 ± 12	65 ± 11	0.11
Familial history of CAD (%)	9 (14)	5 (15)	4 (13)	0.54
Preinfarction angina pectoris (%)	24 (38)	16 (50)	8 (26)	0.059
Killip class	1.1 ± 0.4	1.0 ± 0.1	1.2 ± 0.6	0.18
Coronary risk factors				
Diabetes mellitus (%)	24 (38)	13 (40)	11 (36)	0.74
Hypertension (%)	39 (62)	21 (65)	18 (60)	0.64
Dyslipidemia (%)	39 (62)	21 (65)	18 (66)	0.93
Smoking (%)	40 (64)	23 (71)	17 (56)	0.21
Laboratory data				
Total cholesterol (mg/dL)	209 ± 38	216 ± 41	200 ± 34	0.10
Triglyceride (mg/dL)	161 ± 96	166 ± 92	155 ± 101	0.65
LDL-cholesterol (mg/dL)	134 ± 31	139 ± 34	129 ± 28	0.25
Scr (mg/dL)	0.84 ± 0.22	0.79 ± 0.16	0.89 ± 0.26	0.09
Plasma glucose level (mg/dL)	197 ± 88	196 ± 100	197 ± 74	0.98
HbA1c (%)	6.6 ± 1.8	6.7 ± 2.1	6.4 ± 1.3	0.42

Values are mean ± 1 SD or number (%). MO = microvascular obstruction; CAD = coronary artery disease; LDL = low-density lipoprotein; Scr = serum creatinine; HbA1c = glycosylated hemoglobin concentration.

temporal resolution, 20 ms. Delayed enhancement sequences were acquired after the injection of a 0.2 mmol/kg body weight of gadopentetate dimeglumine (Gd-DTPA; Magnevist, Berlex Laboratories, Montville, NJ), with the following parameters: repetition time, 3.8 ms; echo time, 1.2 ms; slice thickness, 5 mm; no gap between slice; flip angle, 15; field of view, 380 × 380 mm; matrix, 224 × 256. Images were acquired 10 min after Gd-DTPA injection. The inversion time was manually adjusted between 200–350 ms to null the signal from normal myocardium.

All examinations were transferred to a computer workstation. Left ventricular (LV) end-diastolic volume, LV end-systolic volume, and LV ejection fraction were measured on cine images using standard techniques [24], and analyzed by semi-automated software for volumetric analysis (Philips Healthcare, Best, The Netherlands).

The areas of myocardial infarction were defined as hyperintense areas in the LV myocardial wall, supplied by the infarct-related artery and MO as a hypo-enhanced area within a hyper-enhanced infarct area on the late gadolinium enhancement (LGE) images [8]. Left ventricular myocardial volume, infarct volume, and MO volume were semi-automatically measured based on short-axis images using an image-processing software (Virtual Place, AZE, Tokyo, Japan). The quantitative extent of LGE was derived from its full-width with the half-maximum thresholding technique [25]. The percentage infarct size (%IS) was calculated as follows: total infarct volume divided by total myocardial volume. The quantitative extent of MO was semi-automatically calculated as the 3D-volume of the hypo-enhanced area in the hyper-enhanced myocardium, and MO was included in the calculation of total infarct size. The percentage MO (%MO) was calculated as follows: total MO volume divided by total myocardial volume. Patients with MO were defined as those who visually showed the presence of MO and quantitatively showed a %MO > 0. All images were analyzed by two experienced observers blinded to the clinical data. In case of disagreement of visual assessments, consensus interpretation was appended.

2.5. Patient classification

Patients were divided into 2 groups according to the visual assessment from CMR imaging as follows: 32 patients showing MO (MO group); and 30 who did not show MO (non-MO group).

2.6. Statistical analysis

Continuous variables were expressed as mean ± standard deviation (SD). Comparisons of continuous variables between groups were performed with the unpaired t-test. Categorical variables were compared with the chi-square test. The correlation analysis was performed with Pearson's correlation methods. Binary logistic regression analysis was performed to reveal the determinants of the presence of MO. Using statistically significant variables ($p < 0.05$) with the univariate anaysis, the multivariate analysis was applied. An IBM SPSS Statistics 20 software (SPSS, Chicago, IL) was used for the statistical analyses. A p value of <0.05 was considered statistically significant.

3. Results

3.1. Patient characteristics

The comparisons of baseline characteristics in all patients and each group are shown in Table 1. No significant differences in terms of age, sex, familial history of coronary artery disease, preinfarction angina pectoris, Killip class, diabetes mellitus, hypertension, dyslipidemia, and smoking were observed between the 2 groups. No significant differences were observed in total cholesterol, triglyceride, low-density lipoprotein cholesterol, serum creatinine levels and plasma glucose levels on admission, or glycosylated hemoglobin concentrations.

3.2. Angiographic demonstrations

The comparisons of angiographic characteristics of all patients and each group are shown in Table 2. A significant difference was observed in infarct-related arteries between the 2 groups. No significant differences were observed in the number of diseased vessels, the onset-to-reperfusion time, and the door-to-reperfusion time between the 2 groups. The peak CK value was significantly higher in the MO group than in the non-MO group (4428 ± 1726 vs. 2082 ± 1699 IU/L, $p < 0.001$). The percentage of patients showing no-reflow or slow-flow were significantly higher in the MO group than in the non-MO group (40% vs. 10%, $p = 0.006$). The percentage of patients undergoing distal protections were similar between the 2 groups.

Table 2
Angiographic characteristics of patients with and without MO.

Parameter	All patients ($n=62$)	MO group ($n=32$)	Non-MO group ($n=30$)	p value
Infarct-related artery				0.04
LAD, (%)	29 (46)	20 (62)	9 (30)	
LCX, (%)	6 (9)	2 (6)	4 (13)	
RCA, (%)	27 (43)	10 (31)	17 (56)	
No. of diseased vessels				0.29
One, (%)	43 (69)	25 (78)	18 (60)	
Two, (%)	14 (22)	5 (15)	9 (30)	
Three, (%)	5 (8)	2 (6)	3 (10)	
Results of reperfusion				
Onset to reperfusion, (min)	256 ± 212	262 ± 253	249 ± 162	0.82
Door to reperfusion, (min)	86 ± 41	89 ± 43	83 ± 40	0.59
Peak CK value, (IU/L)	3292 ± 2069	4428 ± 1726	2082 ± 1699	<0.001
No-reflow or slow flow, (%)	16 (25)	13 (40)	3 (10)	0.006
Distal protection, (%)	5 (8)	3 (9)	2 (6)	0.53

Values are mean ± SD or number (%). MO = microvascular obstruction; LAD = left anterior descending artery; LCX = left circumflex artery; RCA = right coronary artery; CK = creatine phosphokinase.

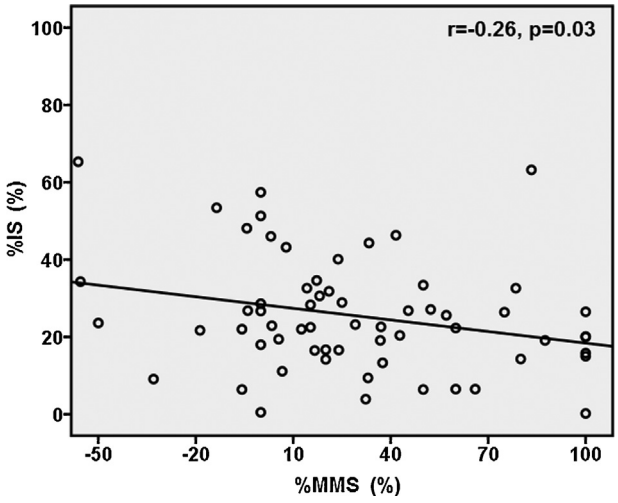

Fig. 1. Relationship between scintigraphic mismatch and infarct size. The percentage mismatch score (%MMS) significantly correlated with the percentage infarct size (%IS).

3.3. Comparison of CMR with dual SPECT findings

The ^{201}Tl and ^{123}I-BMIPP scores significantly correlated with %IS ($r=0.48$, $p<0.001$; $r=0.43$, $p<0.001$, respectively). The %MMS significantly correlated with %IS ($r=-0.26$, $p=0.03$; Fig. 1). ^{201}Tl and ^{123}I-BMIPP defect scores were significantly greater in the MO group than in the non-MO group (18.5 ± 9.0 vs. 5.8 ± 6.1, $p<0.001$; 20.6 ± 8.2 vs. 9.7 ± 7.5, $p<0.001$, respectively; Table 3), and %MMS was significantly greater in the non-MO group than in the MO group (45.4 ± 42.4 vs. 13.3 ± 28.0, $p=0.001$; Table 3).

The ^{201}Tl and ^{123}I-BMIPP scores significantly correlated with %MO ($r=0.68$, $p<0.001$; $r=0.57$, $p<0.001$, respectively; Fig. 2A and B), and %MMS significantly correlated with %MO ($r=-0.45$, $p<0.001$; Fig. 2C).

Table 3
Scintigraphic characteristics of patients with and without MO.

Parameter	All patients ($n=62$)	MO group ($n=32$)	Non-MO group ($n=30$)	p value
^{201}Tl score	12.4 ± 10.0	18.5 ± 9.0	5.8 ± 6.1	<0.001
^{123}I-BMIPP score	15.4 ± 9.5	20.6 ± 8.2	9.7 ± 7.5	<0.001
%MMS (%)	28.8 ± 39.0	13.3 ± 28.0	45.4 ± 42.4	0.001

Values are mean ± 1 SD. MO = microvascular obstruction; %MMS = percentage mismatch score.

3.4. Comparisons of findings on CMR imaging between patients with and without MO

As shown in Table 4, the %IS was significantly greater in the MO group than in the non-MO group (32.2 ± 13.8% vs. 18.3 ± 12.1%, $p<0.001$). The LV ejection fraction was significantly greater in the non-MO group than in the MO group (51.5 ± 7.6% vs. 42.8 ± 8.8%, $p<0.001$). LV end-diastolic volume and LV end-systolic volume were significantly greater in the MO group than in the non-MO group (128.0 ± 34.4 mL vs. 105.1 ± 32.0 mL, $p=0.009$; 74.9 ± 28.4 mL vs. 52.1 ± 20.3 mL, $p=0.001$, respectively).

3.5. Binary logistic regression analysis for the presence of MO

On binary logistic regression analysis after adjustment for the presence of MO, the %MMS proved to be an independent predictor for MO (OR 0.97, 95%CI 0.94–0.99, $p=0.02$; Table 5).

3.6. Case presentations

The representative 4 cases are presented in Fig. 3A–D.

4. Discussion

In the present study, 52% of the patients who successfully underwent PCI exhibited MO in the infarct areas. Patients with MO showed a higher peak CK level, a larger infarct size, a worse LV ejection fraction, and a smaller %MMS than those without MO. A significant inverse correlation was observed between %MMS and %MO as well as %IS. Our results reinforce the contention that MO detected by CMR imaging after AMI is to be considered an unfavorable structural abnormality even when PCI is successfully conducted.

The MO on CMR imaging is considered to consist of the following mechanisms. In experimental studies [26,27], the territory injured by prolonged ischemia is composed primarily of nonviable myocardial tissue in which myocytes die first, eventually followed by necrosis of the endothelial cells in intramyocardial capillaries. Particularly at the center of the infarct area, myocites and capillaries may undergo necrosis simultaneously because of profound and sustained ischemia. In such situations,

Table 4
CMR characteristics of patients with and without MO.

Parameter	All patients (n = 62)	MO group (n = 32)	Non-MO group (n = 30)	p value
%IS (%)	25.5 ± 14.7	32.2 ± 13.8	18.3 ± 12.1	<0.001
LV ejection fraction (%)	46.3 ± 11.0	42.8 ± 8.8	51.5 ± 7.6	<0.001
LV end-diastolic volume (mL)	116.9 ± 34.9	128.0 ± 34.4	105.1 ± 32.0	0.009
LV end-systolic volume (mL)	63.8 ± 27.2	74.9 ± 28.4	52.1 ± 20.3	0.001

Values are mean ± 1 SD. MO = microvascular obstruction; IS = infarct size; LV = left ventricular.

Table 5
Binary logistic regression analysis for the presence of MO.

Variable	Univariate		Multivariate	
	Unadjusted OR (95% CI)	p value	Adjusted OR (95% CI)	p value
Peak CK value, (IU/L)	1.001 (1.00–1.001)	<0.001	1.00 (1.000–1.001)	0.11
LV ejection fraction on CMR (%)	0.87 (0.80–0.94)	0.001	0.90 (0.81–1.00)	0.07
%IS (%)	1.09 (1.03–1.15)	0.001	1.06 (0.99–1.13)	0.08
%MMS (%)	0.97 (0.95–0.99)	0.003	0.97 (0.94–0.99)	0.02

OR = odds ratio; CI = confidence interval; MO = microvascular obstruction; CK = creatine phosphokinase; LV = left ventricular; %MMS = percentage mismatch score.

capillaries are obstructed by dying blood cells and debris. Eventually, the infarct core is not reperfused, although epicardial blood flow is adequately restored. Since contrast media fails to influx into the central infarct core because of capillary obstruction, the hypo-enhanced areas within the hyper-enhanced areas are quite viewable on the delayed enhanced images. Areas showing MO correspond to the "no-reflow" or "slow-reflow" regions [28]. The presence of MO after AMI leads to poor global LV function even in the early postinfarct phase. Also, contrast-enhanced ultrasonic echocardiography enables the detection of MO [29,30]. However, echocardiography is an operator-dependent examination, and results are often affected by the attenuation involved in the body mass. In addition, considerable skill is required for evaluating the presence of MO. Therefore, operator-independent CMR imaging may be a better examination for detecting MO than echocardiography.

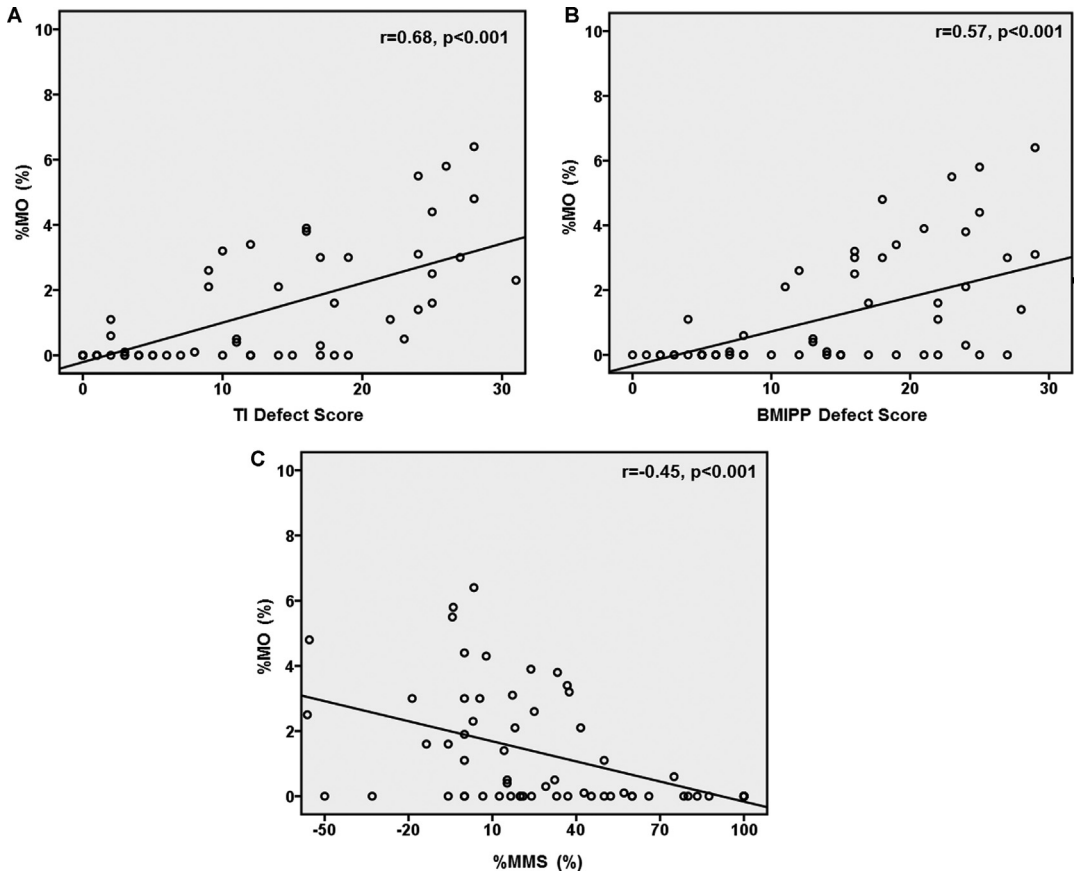

Fig. 2. Relationship between MO and scintigraphic scores. (A) The ^{201}Tl score significantly correlated with the percentage MO (%MO). (B) The ^{123}I-BMIPP score significantly correlated with the %MO. (C) The %MMS significantly correlated with the %MO.

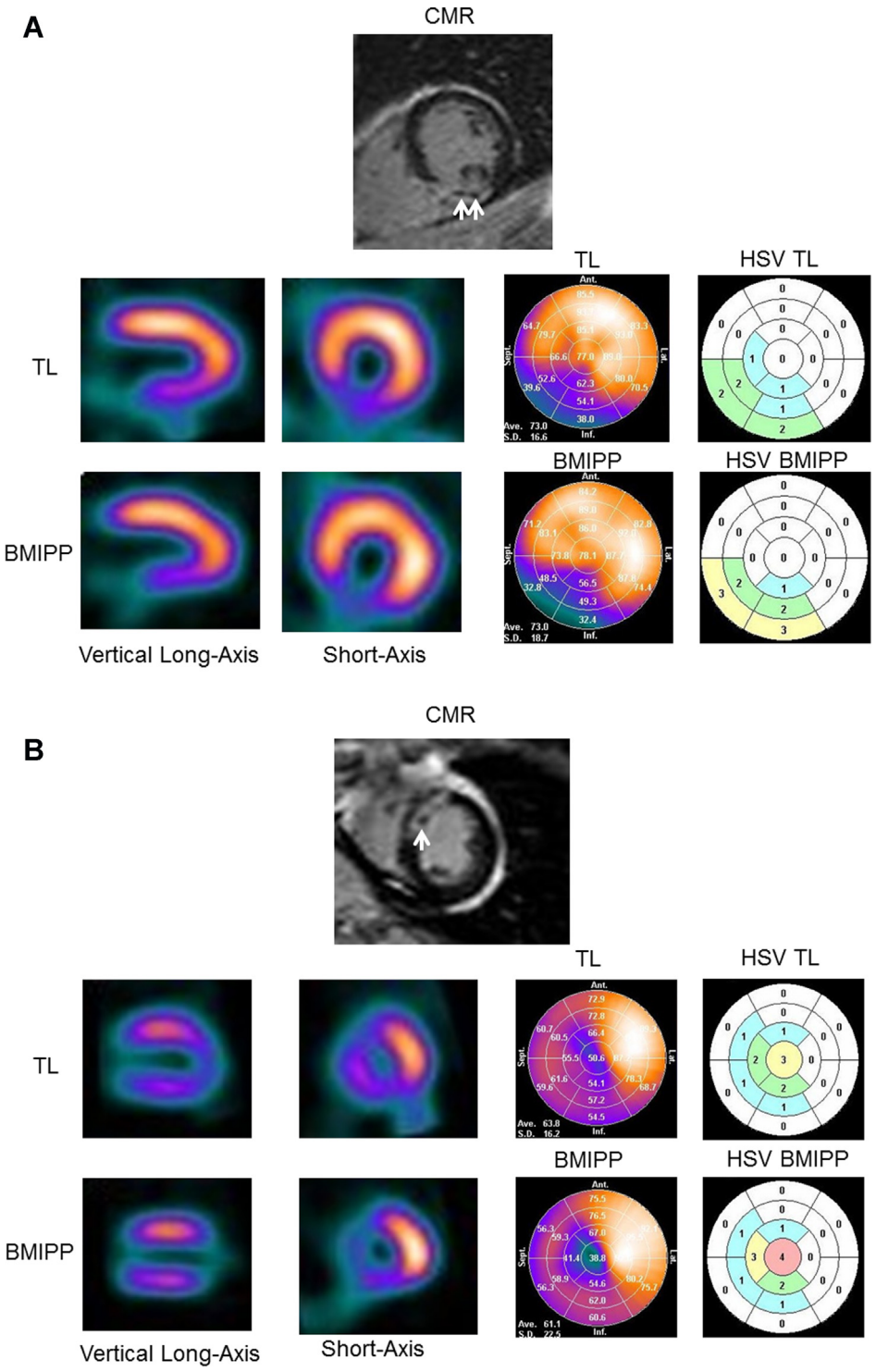

Fig. 3. Representative cases of each group. (A) Cardiac magnetic resonance (CMR) image, dual SPECT, polar map, and Heart Score View (HSV) of a 42-year-old male with acute inferior infarction. The peak CK is 4748 IU/L. Microvascular obstruction (MO) is observed within the infarct area (arrow). The percentage infarct size (%IS) and percentage MO (%MO) are 30.6% and 2.1%, respectively. The total defect score of ^{201}Tl and ^{123}I-BMIPP are 9 and 11, indicating a concordant defect. The %MMS is 18.1%. (B) CMR image, dual SPECT, polar map, and HSV of a 75-year-old male with acute anterior infarction. The peak CK is 3110 IU/L. MO is observed within the infarct area (arrow). The %IS and %MO are 28.3% and 0.5%, respectively. The total defect score of ^{201}Tl and ^{123}I-BMIPP are 11 and 13, indicating a concordant defect. The %MMS is 15.3%. (C) CMR image, dual SPECT, polar map, and HSV of a 64-year-old male with acute inferior infarction. The peak CK is 1636 IU/L. MO is not observed within the infarct area. The %IS is 14.3%. The total defect score of ^{201}Tl and ^{123}I-BMIPP are 1 and 5, indicating a discordant defect on both images. The %MMS is 80%. (D) CMR image, dual SPECT, polar map, and HSV of a 46-year-old male with acute anterior infarction. The peak CK is 9616 IU/L. MO is not observed within the infarct area. The %IS is 32.6%. The total defect score of ^{201}Tl and ^{123}I-BMIPP are 3 and 14, indicating a discordant defect on both images. The %MMS is 78.5%.

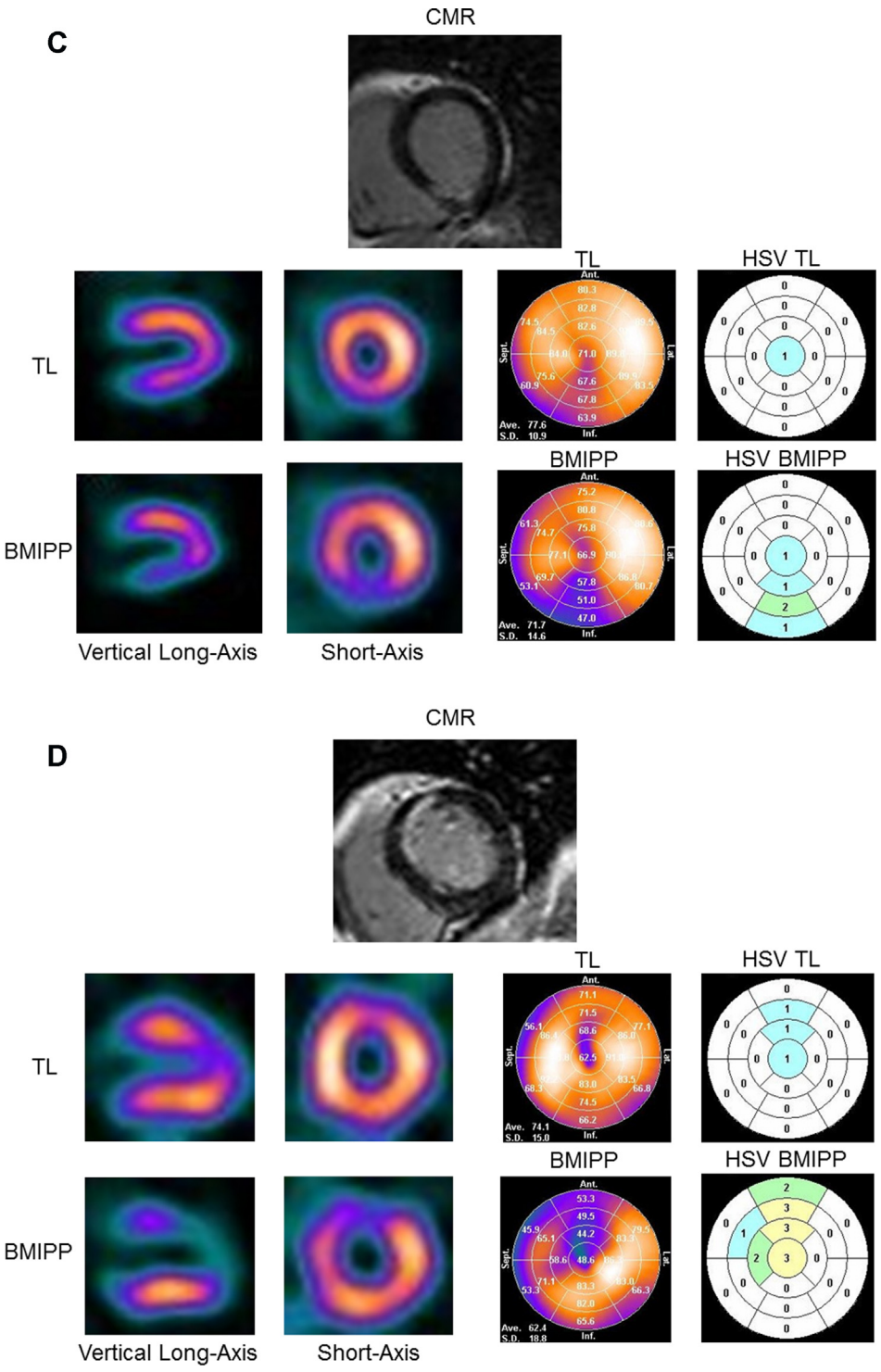

Fig. 3. (*Continued*).

An iodine-123 radiolabeled tracer, ^{123}I-BMIPP has been developed as a clinical-use tracer for visualizing myocardial fatty acid metabolism. ^{123}I-BMIPP is transported into the myocardium in a way similar to native free-fatty acid. It is slowly metabolized by β-oxidation and is characterized by a prolonged retention in the myocardium, serving as a useful radiolabeled tracer for SPECT imaging [31]. In combination with a flow tracer, ^{201}Tl, ^{123}I-BMIPP uptake is more reduced compared to ^{201}Tl uptake in areas at risk in the acute or subacute phase of AMI patients undergoing emergency revascularization [32]. The discordant ^{123}I-BMIPP uptake is related to the impaired but viable myocardium. A flow-metabolism mismatch on both images is considered to be favorable evidence associated with the further improvement in myocardial function [12,13]. Alternatively, AMI patients showing a concordant defect on ^{201}Tl/^{123}I-BMIPP dual SPECT have worse outcomes than those without it [17–20]. Therefore, ^{123}I-BMIPP SPECT in combination with ^{201}Tl SPECT may provide useful information regarding myocardial cellular reversibility in areas at risk in the relatively early phase after AMI [18].

Flow-metabolism mismatch was more frequently observed in AMI patients without MO than in those with it. Binary logistic regression analysis revealed that the %MMS was an independent predictor for MO after AMI. On the other hand, the peak CK levels, LV ejection fraction, and %IS did not predict it. Myocardial ^{201}Tl/^{123}I-BMIPP dual scintigraphy may be an important physiological procedure for confirming the presence of MO in AMI patients after emergency revascularization.

In the present study, MO on CMR imaging was frequently observed in patients showing a concordant defect on ^{201}Tl/^{123}I-BMIPP dual SPECT. A concordant defect of flow-metabolic dual tracers is associated with irreversible myocardial damage in the infarct area after AMI, leading to poor functional recovery followed by worse outcome [16–19]. Microvascular obstruction after revascularization is reportedly associated with poor prognosis [10]. In line with previous studies [4,5], MO after AMI is often observed in patients exhibiting slow-flow or no-reflow, and has been reconfirmed to be unfavorable structural damage in comparison with myocardial ^{201}Tl/^{123}I-BMIPP dual scintigraphy. MO appears irrespective of the success of PCI or the onset-to-reperfusion time. Aggressive strategies to prevent myocardial remodeling are required, even for AMI patients who successfully undergo PCI but show MO on the LGE images in the relatively early stage after AMI. In addition, noninvasive evaluation of MO using CMR imaging may be clinically useful for assuring the prognosis of AMI patients at the early stage after AMI.

5. Conclusions

First of all, we suggest that there is a relationship between myocardial structural abnormalities on CMR and physiological characteristics on dual SPECT in AMI patients. MO is associated with irreversible physiological myocardial damage. On the other hand, patients without MO exhibit physiological residual viability on areas at risk. Our results reinforce the contention that MO is an important unfavorable structural abnormality associated with irreversible myocardial damage in AMI patients who undergo successful reperfusion therapies, in comparison with myocardial dual scintigraphy.

Conflict of interest

The authors declare that they have no conflicts of interest.

Acknowledgements

We thank Morikatsu Matsuda, Nobuhiro Yoshida, and Koji Mizutani, radiological technicians, for their technical assistance with the CMR and scintigraphic studies.

References

[1] Iwakura K, Ito H, Takiuchi S, Taniyama Y, Nakatsuchi Y, Negoro S, et al. Alternation in the coronary blood flow velocity pattern with no reperfused acute myocardial infarction. Circulation 1996;94:1269–75.
[2] Iwakura K, Ito H, Kawano S, Shinani Y, Yamamoto K, Kato A, et al. Predictive factors for development of the no-reflow phenomenon in patients with reperfused anterior wall acute myocardial infarction. J Am Coll Cardiol 2001;38:472–7.
[3] Lima JA, Judd RM, Bazille A, Schulman SP, Atalar E, Zerhouni EA. Regional heterogeneity of human myocardial infarcts demonstrated by contrast-enhanced MRI. Potential mechanisms. Circulation 1995;92:1117–25.
[4] Hombach V, Grebe O, Merkle N, Waldenmaier S, Höher M, Kochs M, et al. Sequelae of acute myocardial infarction regarding cardiac structure and function and their prognostic significance as assessed by magnetic resonance imaging. Eur Heart J 2005;26:549–57.
[5] Wu KC, Zerhouni EA, Judd RM, Lugo-Olivieri CH, Barouch LA, Schulman SP, et al. Prognostic significance of microvascular obstruction by magnetic resonance imaging in patients with acute myocardial infarction. Circulation 1998;97:765–72.
[6] Gerber BL, Rochitte CE, Melin JA, McVeigh ER, Bluemke DA, Wu KC, et al. Microvascular obstruction and left ventricular remodeling early after acute myocardial infarction. Circulation 2000;101:2734–41.
[7] Raff GL, O'Neill WW, Gentry RE, Dulli A, Bis KG, Shetty AN, et al. Microvascular obstruction and myocardial function after acute myocardial infarction: assessment by using contrast-enhanced cine MR imaging. Radiology 2006;240:529–36.
[8] Nijveldt R, Hofman MB, Hirsch A, Beek AM, Umans VA, Algra PR, et al. Assessment of microvascular obstruction and prediction of short-term remodeling after acute myocardial infarction: cardiac MR imaging study. Radiology 2009;250:363–70.
[9] Kidambi A, Mather AN, Motwani M, Swoboda P, Uddin A, Greenwood JP, et al. The effect of microvascular obstruction and intramyocardial hemorrhage on contractile recovery in reperfused myocardial infarction: insights from cardiovascular magnetic resonance. J Cardiovasc Magn Reson 2013;15:58.
[10] Bolognese L, Carrabba N, Parodi G, Santoro GM, Buonamici P, Cerisano G, et al. Impact of microvascular dysfunction on left ventricular remodeling and long-term clinical outcome after primary coronary angioplasty for acute myocardial infarction. Circulation 2004;109:1121–6.
[11] Kropp J, Jorgens M, Glanzer KP, Luderitz B, Biersack HJ, Knapp FF. Evaluation of ischemia and myocardial viability in patients with coronary artery disease (CAD) with iodone-123 labeled 15-(p-iodophenyl)-3-RS-methylpentadecanoic acid (BMIPP). Ann Nucl Med 1993;7(Suppl. II):93–100.
[12] Tamaki N, Kawamoto M, Yonekura Y, Fujibayashi Y, Takahashi N, Konishi J, et al. Regional metabolic abnormality in relation to perfusion and wall motion in patients with myocardial infarction: assessment with emission tomography using an iodinated branched fatty acid analog. J Nucl Med 1992;33:659–67.
[13] Matsunari I, Saga T, Taki J, Akashi Y, Hirai J, Wakasugi T, et al. Kinetics of iodine-123-BMIPP in patients with prior myocardial infarction: assessment with dynamic rest and stress images compared with stress thallium-201 SPECT. J Nucl Med 1994;35:1279–85.
[14] De Geeter F, Franken PR, Knapp Jr FF, Bossuyt A, Bossuyt A. Relationship between blood flow and fatty acid metabolism in subacute myocardial infarction: a study by means of ^{99m}Tc-Sestamibi and ^{123}I-beta-methyl-iodo-phenyl pentadecanoic acid. Eur J Nucl Med 1994;21:283–91.
[15] Shimonagata T, Nanto S, Kusuoka H, Ohara T, Inoue K, Yamada S, et al. Metabolic changes in hibernating myocardium after percutaneous transluminal coronary angioplasty and the relation between recovery in left ventricular function and free fatty acid metabolism. Am J Cardiol 1998;82:559–63.
[16] Nakata T, Hashimoto A, Kobayashi H, Miyamoto K, Tsuchihashi K, Miura T, et al. Outcome significance of thallium-201 and iodine-123-BMIPP perfusion-metabolism mismatch in preinfarction angina. J Nucl Med 1998;39:1492–9.
[17] Chikamori T, Yamashina A, Hida S, Nishimura T. Diagnostic and prognostic value of BMIPP imaging. J Nucl Cardiol 2007;14:111–25.
[18] Hashimoto A, Nakata T, Nagao K, Kobayashi H, Hase M, Yoshioka N, et al. Prediction of left ventricular functional recovery in patients with acute myocardial infarction using single photon emission computed tomography with thallium-201 and iodine-123-beta-methyl-p-iodophenyl-pentadecanoic acid. J Cardiol 1995;26:59–68.
[19] Ito T, Tanouchi J, Kato J, Morioka T, Nishino M, Iwai K, et al. Recovery of impaired left ventricular function in patients with acute myocardial infarction is predicted by the discordance in defect size on ^{123}I-BMIPP and ^{201}Tl SPET images. Eur J Nucl Med 1996;23:917–23.
[20] Nakata T, Kobayashi T, Tamaki N, Kobayashi H, Wakabayashi T, Shimoshige S, et al. Prognostic value of impaired myocardial fatty acid uptake in patients with acute myocardial infarction. Nucl Med Commun 2000;21:897–906.
[21] Ishii H, Ichimiya S, Kanashiro M, Amano T, Imai K, Murohara T, et al. Impact of a single intravenous administration of nicorandil before reperfusion in patients with ST-segment-elevation myocardial infarction. Circulation 2005;112:1284–8.
[22] Beltrame JF. Defining the coronary slow flow phenomenon. Circ J 2012;76:818–20.
[23] Berman DS, Kang X, Gransar H, Gerlach J, Friedman JD, Hayes SW, et al. Quantitative assessment of myocardial perfusion abnormality on SPECT myocardial perfusion imaging is more reproducible than expert visual analysis. J Nucl Cardiol 2009;16:45–53.
[24] Kramer CM, Barkhausen J, Flamm SD, Kim RJ, Nagel E. Standardized cardiovascular magnetic resonance imaging (CMR) protocols, Society for Cardiovascular Magnetic Resonance: Board of Trustees Task Force on Standardized Protocols. J Cardiovasc Magn Reson 2008;10:35.
[25] Amado LC, Gerber BL, Gupta SN, Rettmann DW, Szarf G, Schock R, et al. Accurate and objective infarct sizing by contrast-enhanced magnetic resonance imaging in a canine myocardial infarction model. J Am Coll Cardiol 2004;44:2383–9.
[26] Judd RM, Lugo-Olivieri CH, Arai M, Kondo T, Croisille P, Lima JA, et al. Physiological basis of myocardial contrast enhancement in fast magnetic resonance images of 2-day-old reperfused canine infarcts. Circulation 1995;92:1902–10.
[27] Kim RJ, Chen EL, Lima JA, Judd RM. Myocardial Gd-DTPA kinetics determine MRI contrast enhancement and reflect the extent and severity of myocardial injury after acute reperfused infarction. Circulation 1996;94:3318–26.
[28] Ito H, Maruyama A, Iwakura K, Takiuchi S, Masuyama T, Hori M, et al. Clinical implications of the 'no reflow' phenomenon. A predictor of complications and left ventricular remodeling in reperfused anterior wall myocardial infarction. Circulation 1996;93:223–8.
[29] Ragosta M, Camarano G, Kaul S, Powers ER, Sarembock IJ, Gimple LW. Microvascular integrity indicates myocellular viability in patients with recent

myocardial infarction. New insights using myocardial contrast echocardiography. Circulation 1994;89:2562–9.
[30] Wu KC, Kim RJ, Bluemke DA, Rochitte CE, Zerhouni EA, Becker LC, et al. Quantification and time course of microvascular obstruction by contrast-enhanced echocardiography and magnetic resonance imaging following acute myocardial infarction and reperfusion. J Am Coll Cardiol 1998;32:1756–64.
[31] Dudczak R, Schmoliner R, Angelberger P, Knapp FF, Goodman MM. Structurally modified fatty acids: clinical potential as tracers of metabolism. Eur J Nucl Med 1986;12:S45–8.
[32] Naruse H, Arii T, Kondo T, Morita M, Ohyanagi M, Iwasaki T, et al. Clinical usefulness of iodine 123-labeled fatty acid imaging in patients with acute myocardial infarction. J Nucl Cardiol 1998;5:275–84.